

***X-ray Reflection  
and Reprocessing:***

***Probing Black Holes  
Through Study of  
Fluorescent Iron  
Lines***

**Laura A. Lopez**

**Astro 597**

**20 September 2004**



# *Overview*

- ➔ Introduction
- ➔ Line Production
- ➔ Computing and Modeling  
Line Profiles
- ➔ Iron Lines in AGN
- ➔ Probing Spin via Iron Line  
Observations
- ➔ Future Studies of Iron Lines
- ➔ Conclusions



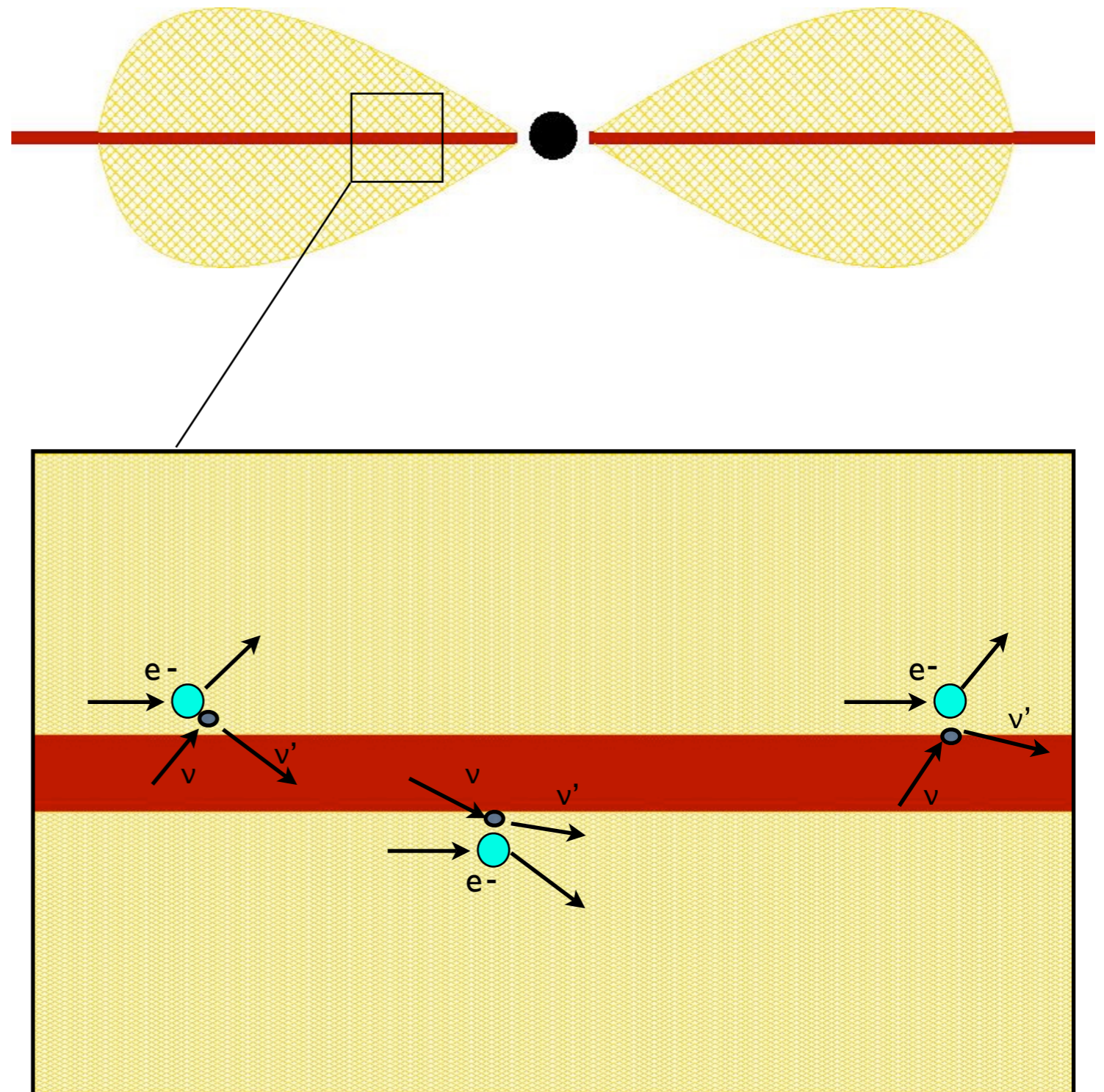
# *Introduccion*

- ➔ In the immediate vicinities of black holes, high-speed matter, electromagnetic fields, and strong gravity effects come together.
- ➔ Direct study of phenomena near black holes is limited because apparent angular scales of even the largest hole event horizons are  $\sim 10^{-6}$  arcsec.
- ➔ Medium- and high-resolution X-ray spectroscopy offers a means to indirectly observe these regions.
- ➔ Fluorescent emission lines resulting from an irradiated cold disk produces  $K\alpha$  iron lines from 6.40-6.97 keV
- ➔ Intrinsically narrow, the iron lines are broadened by Doppler shifts and strong gravity effects.
- ➔ By investigating spectral features in X-ray luminous black holes, scientists can better understand the physics in the immediate vicinity of these systems.



# *Line Production*

- ➔ Assume a cold accretion disk, with uniform density gas.
- ➔ Soft UV/optical photons from the disk will be inverse Compton scattered from high-energy, coronal electrons.
- ➔ These photons gain energy as they are repeatedly IC scattered in the corona
- ➔ Thermal Comptonization of these photons produces a power-law X-ray spectrum

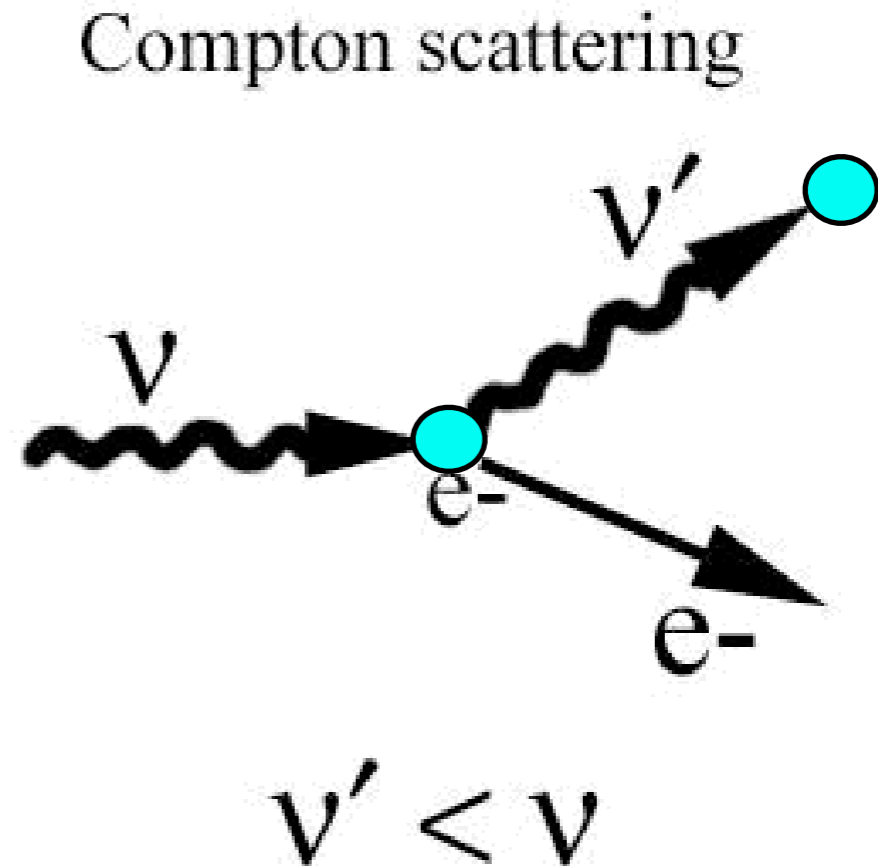


# *Line Production*

- ➔ Resulting high-energy photons re-enter the accretion disk
- ➔ Many possible fates of the incident photons:

## *Fate #1:*

Photon can be Compton scattered by free-electrons from the ionized H and He or by outer electrons of metals.



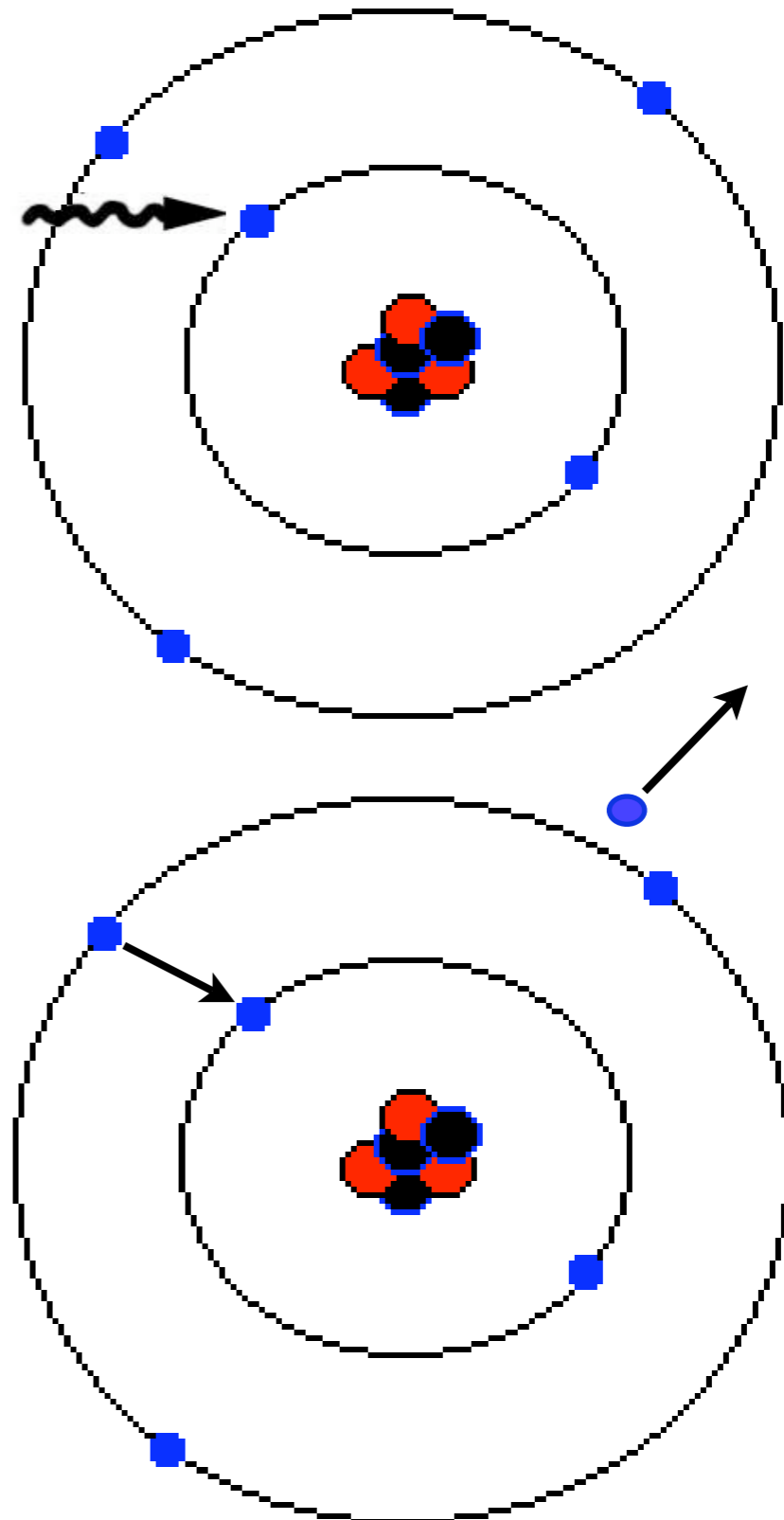
# *Line Production*

- ➔ Resulting high-energy photons re-enter the accretion disk
- ➔ Many possible fates of the incident photons:

## *Fate #2:*

Photon can be photoelectrically absorbed by a neutral atom.

As a result, one K-shell electron will escape, and an L-shell electron will drop into the K-shell

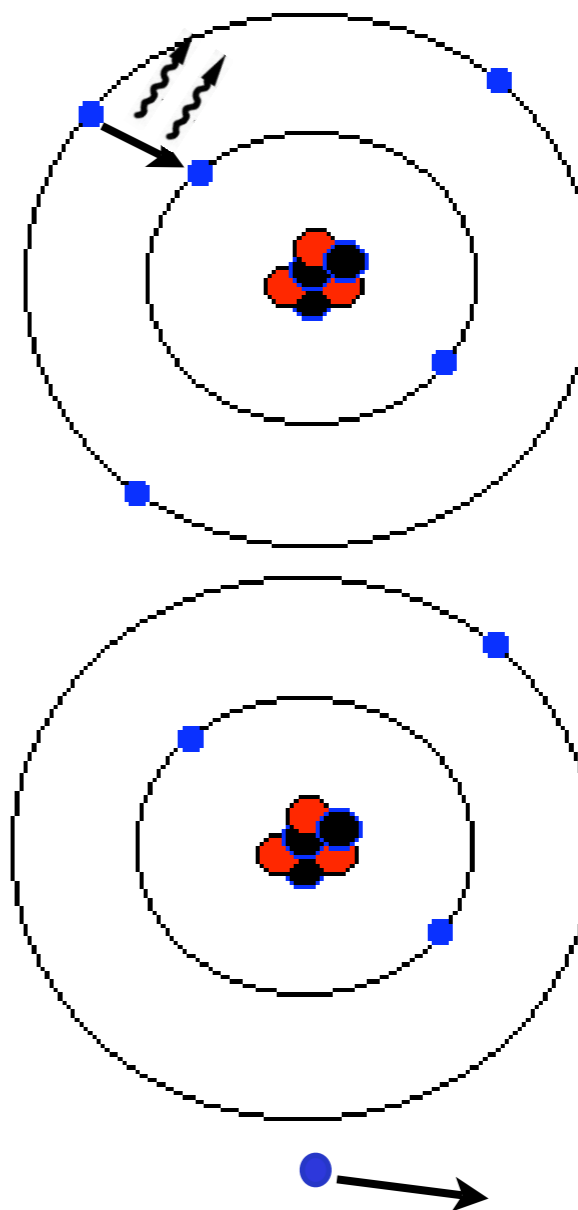


# *Line Production*

This transition creates excess energy which can be released in two ways:

→ **Fluorescence:** Excess energy can be radiated away as a  $K\alpha$  line photon

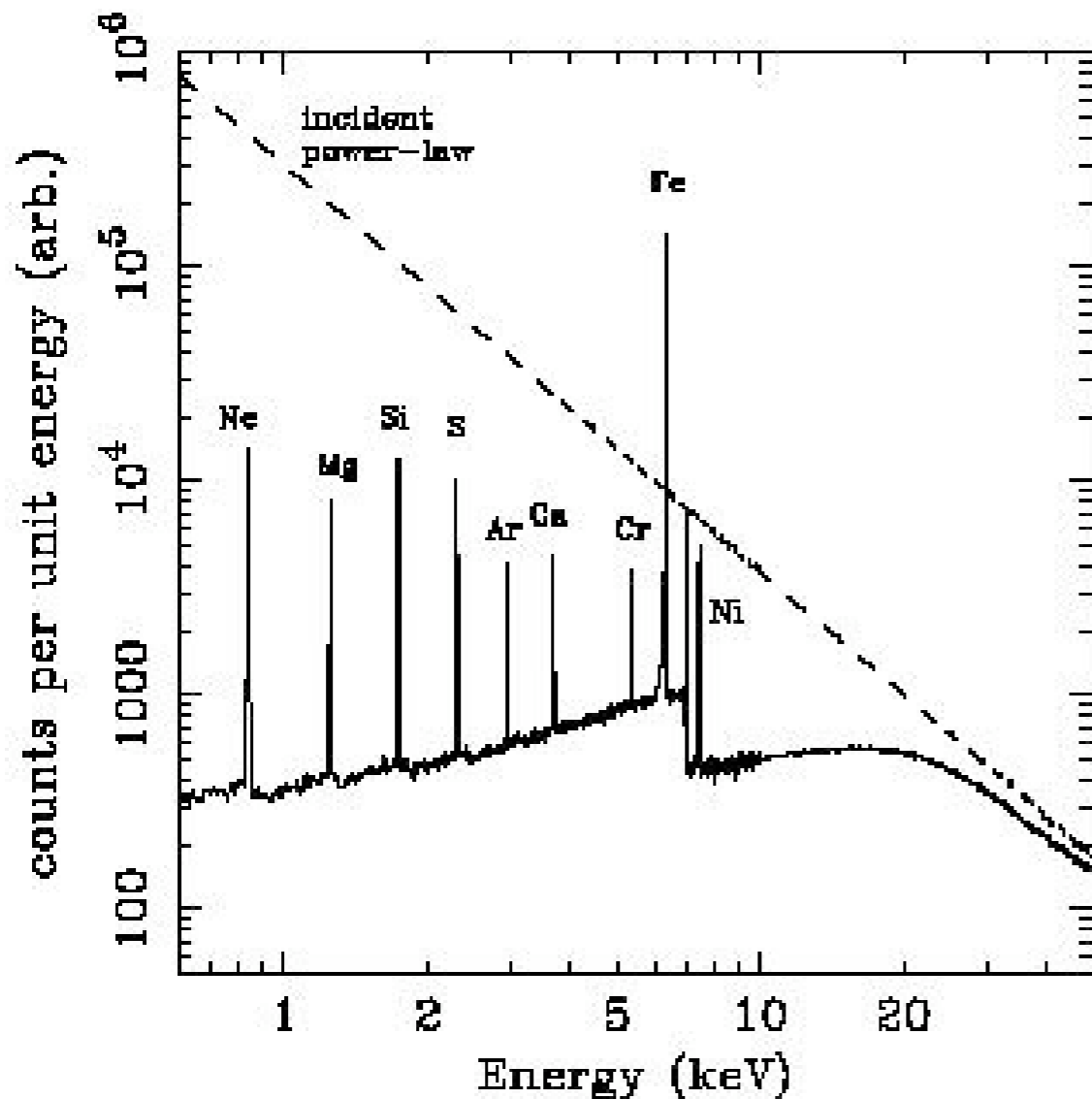
→ **Auger Effect:** Excess energy is carried away via the ejection of a second L-shell electron.



The fluorescent yield of a species determines the probability that an excited ion will de-excite via fluorescence versus the Auger effect.



# *Resulting Spectrum*



- ➔ At soft X-ray energies, reflection is small because of photoabsorption by the metals in the slab.
- ➔ At hard X-ray energies, incident X-rays are Compton back-scattered from the slab.
- ➔ A spectrum of fluorescent emission lines arises from photoionization of metals in the slab.
- ➔ Iron  $K\alpha$  line at 6.40 keV is the most prominent because of its high fluorescent yield and its large cosmic abundance.



# *Effect of Ionization on Spectrum*

➔ The strength of the iron line depends on

- the ionization state of the surface of the accretion disk
- accretion disk geometry
- elemental abundances of the reflecting matter
- the inclination angle of the reflecting material

➔ Amount of ionization is characterized by the ionization parameter,  $\xi$ , where:

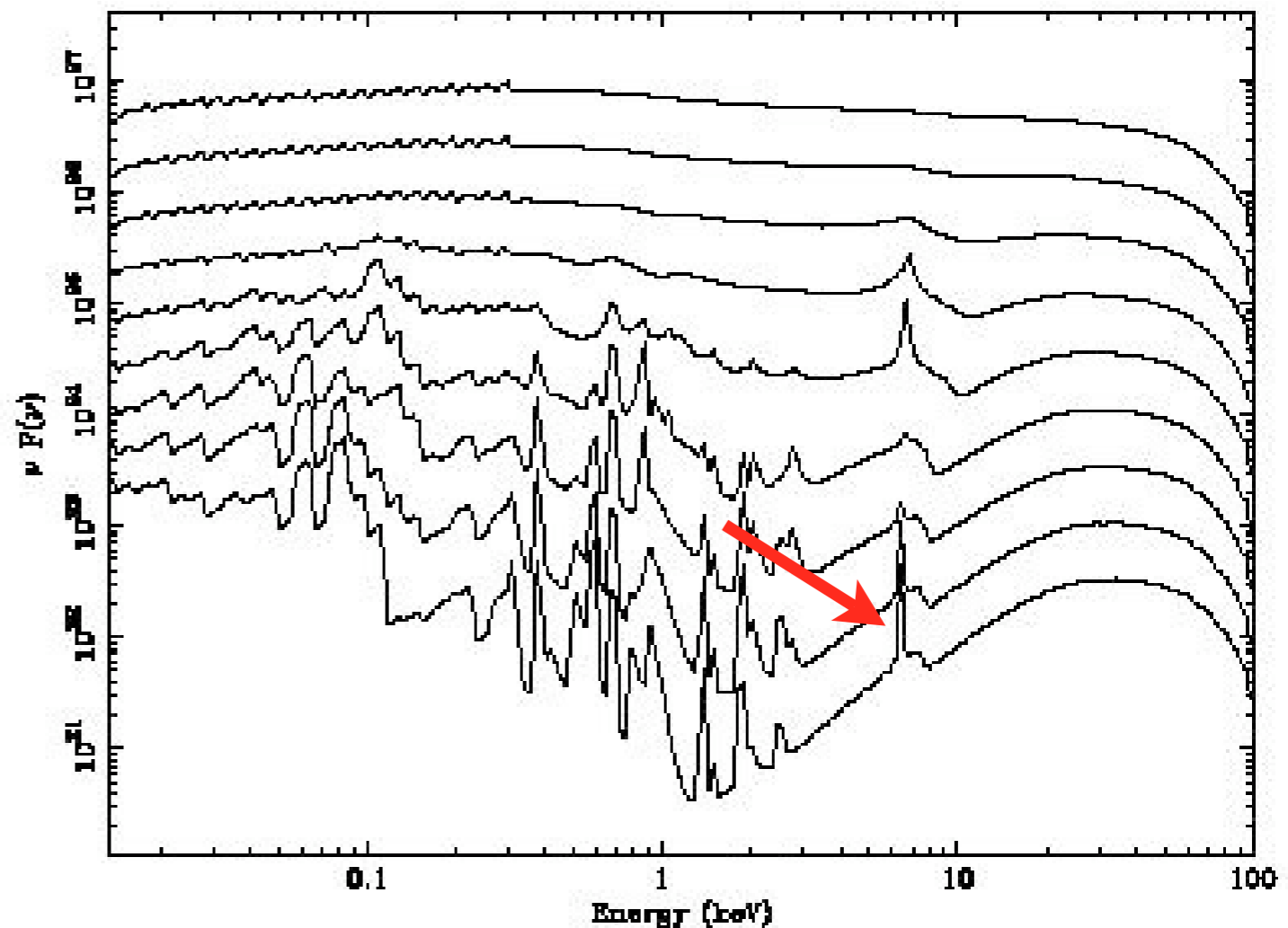
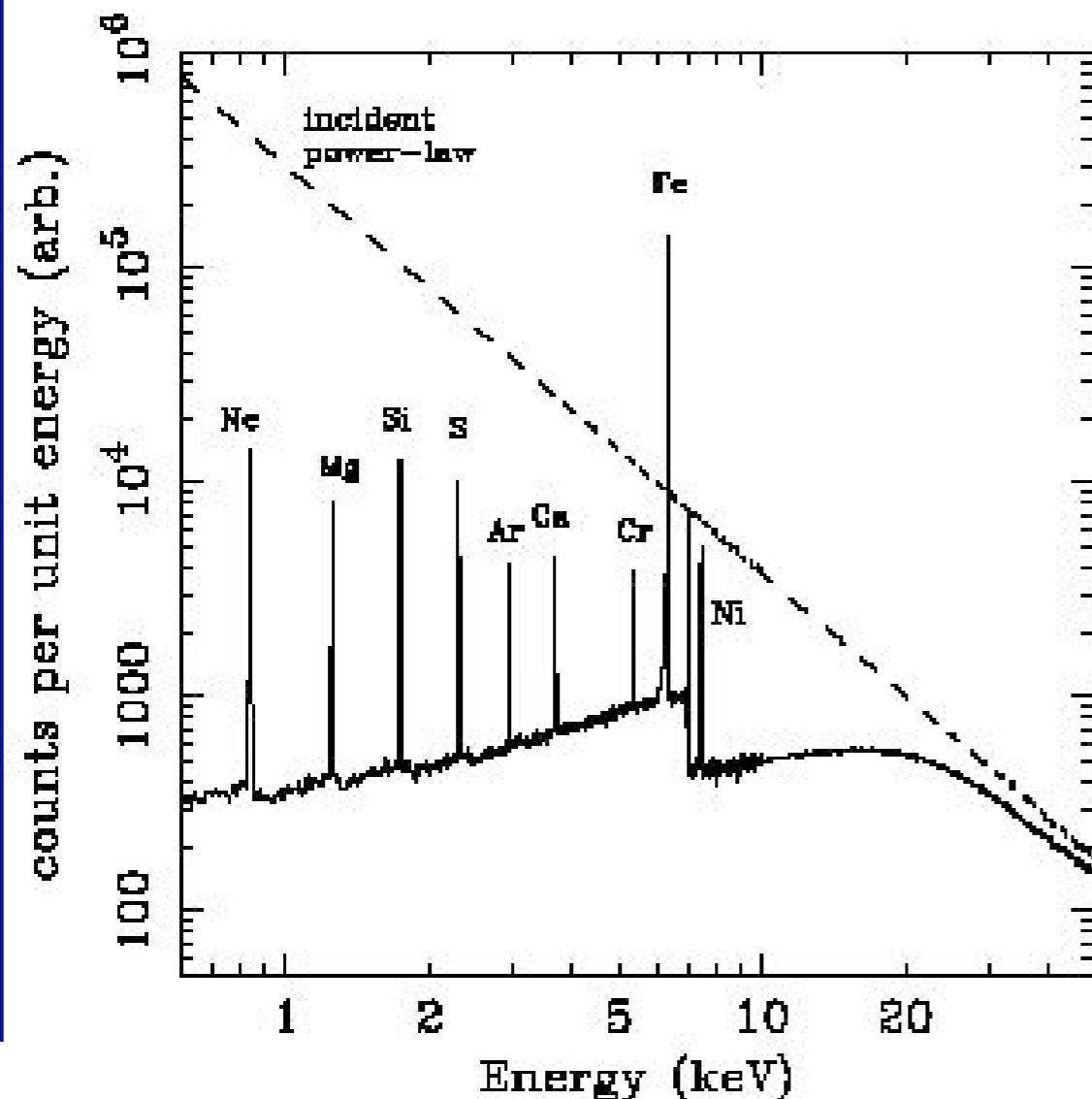
$$\xi (r) = \frac{4\pi F_x(r)}{n (r)}$$

and  $F_x (r)$  is received X-ray flux per unit area of the disk at radius  $r$  and  $n(r)$  is the comoving electron number density.

➔ Assuming uniform density across the disk, iron line emission depends on  $\xi$  and breaks down into four regimes:

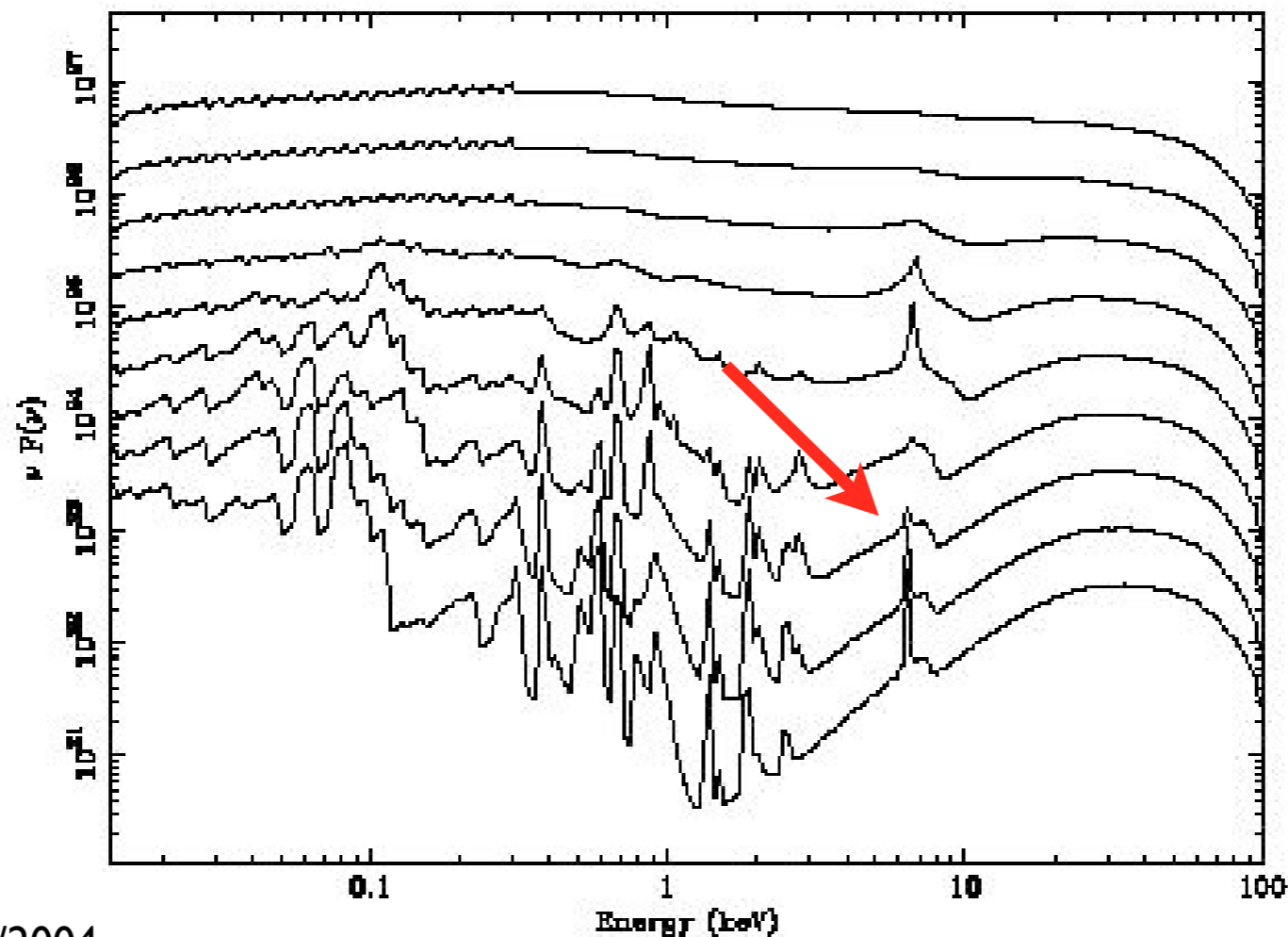
# *Reflection Features for Varying $\xi$*

- ➔ *Case 1:  $\xi < 100 \text{ ergs cm s}^{-1}$  -- cold neutral reflection, weak ionization*
- X-ray reflection resembles that from cold gas containing neutral metals
  - Features include 6.4 keV iron line, a weak iron K-shell edge at 7.1 keV, and a weak Compton back-scattered continuum.



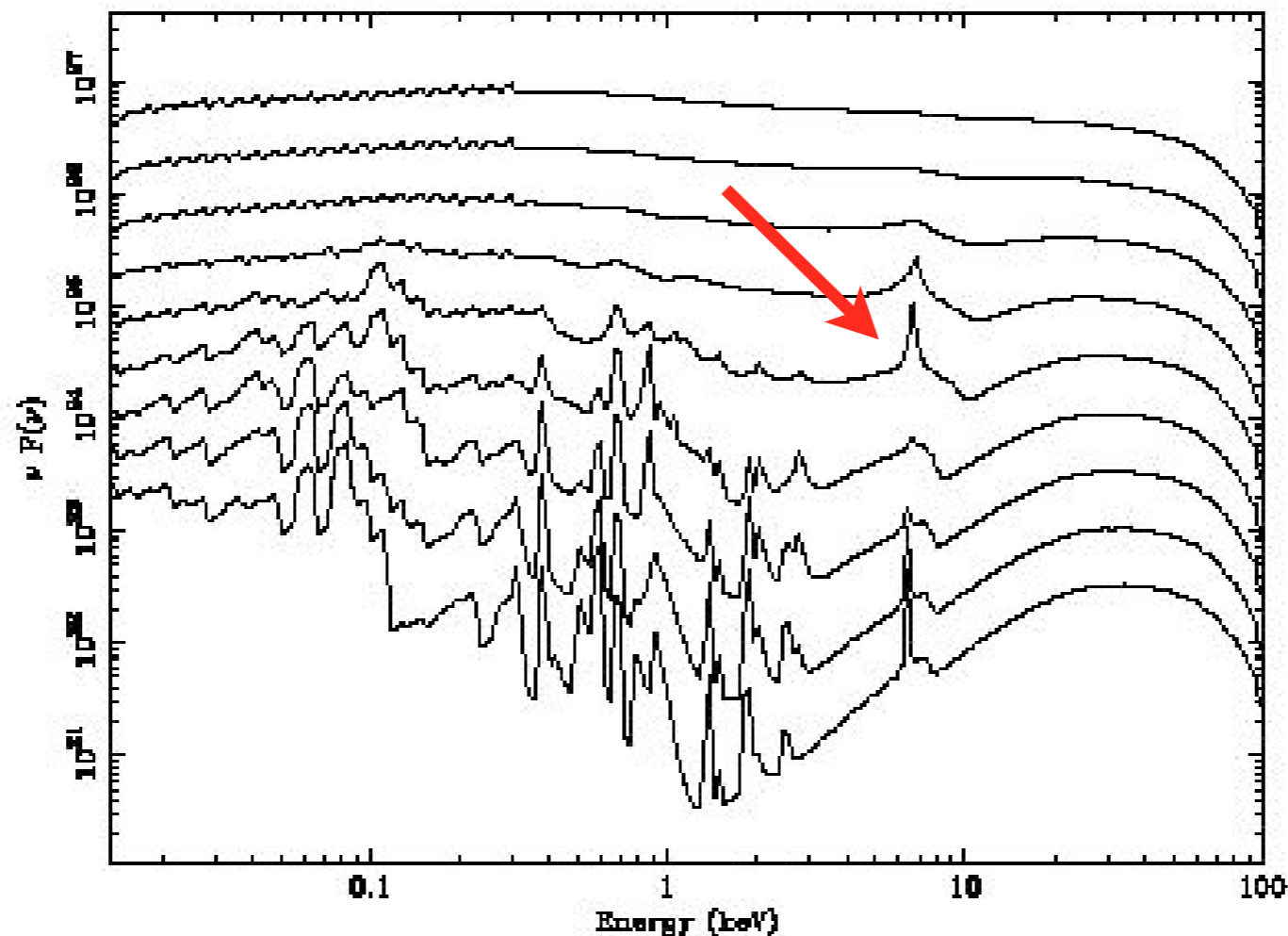
# *Reflection Features for Varying $\xi$*

- ➔ *Case 2:*  $100 \text{ ergs cm s}^{-1} < \xi < 500 \text{ ergs cm s}^{-1}$  -- intermediate ionization
- Iron is in the form Fe XVII - Fe XIII with a vacancy in the L-shell
  - These ions can absorb the  $K\alpha$  line photons. Following absorption, excess energy is released via fluorescence or the Auger effect.
  - Only a few line photons escape the disk, generating a very weak iron line.
  - Spectrum has a moderate iron absorption edge below the iron edge



# *Reflection Features for Varying $\xi$*

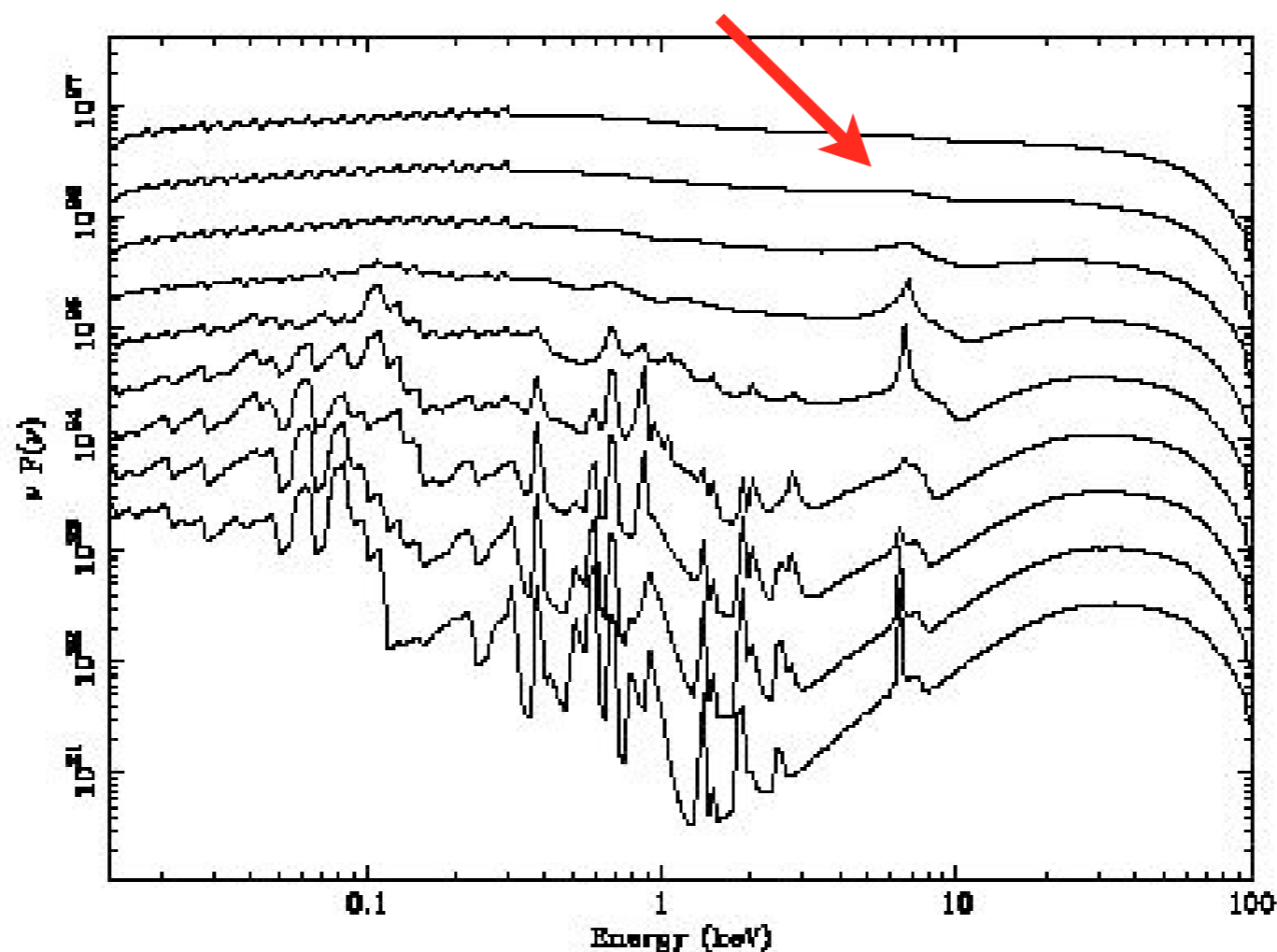
- ➔ *Case 3:  $500 \text{ ergs cm s}^{-1} < \xi < 5000 \text{ ergs cm s}^{-1}$  -- high ionization*
- Ions are too ionized to permit the Auger effect (AE requires 2 L-shell  $e^-$ )
  - Photons can escape the disk, creating a  $K\alpha$  emission of Fe XXV and Fe XVI
  - Compton backscattered continuum significantly contributes to the observed emission at 6 keV, creating a large iron absorption edge.





# *Reflection Features for Varying $\xi$*

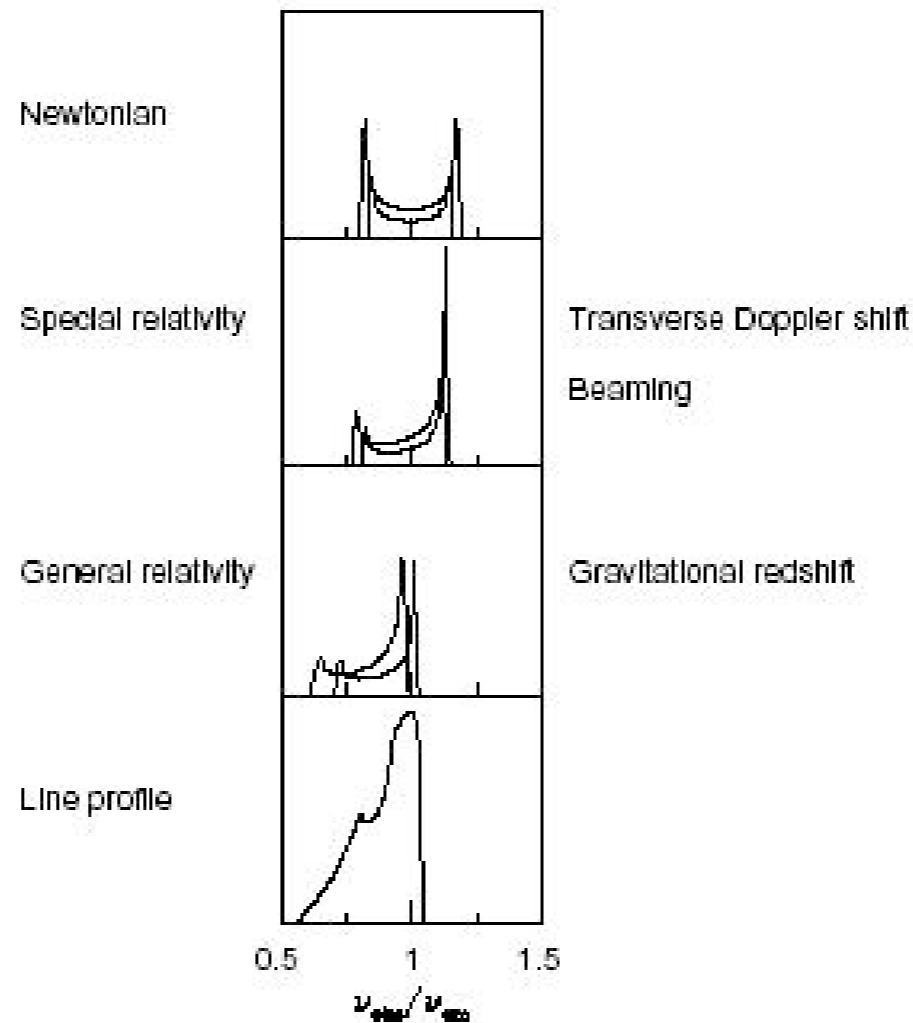
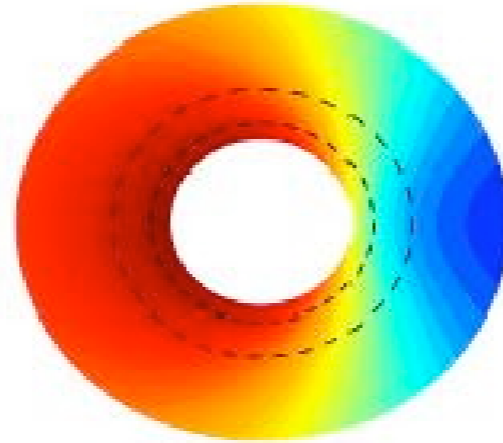
- ➔ *Case 4:  $\xi > 5000$  ergs cm s<sup>-1</sup> -- full ionization*
- The disk is too highly ionized to produce any atomic signatures.
  - No iron emission line or edge is observed.



## *Realistic Models*

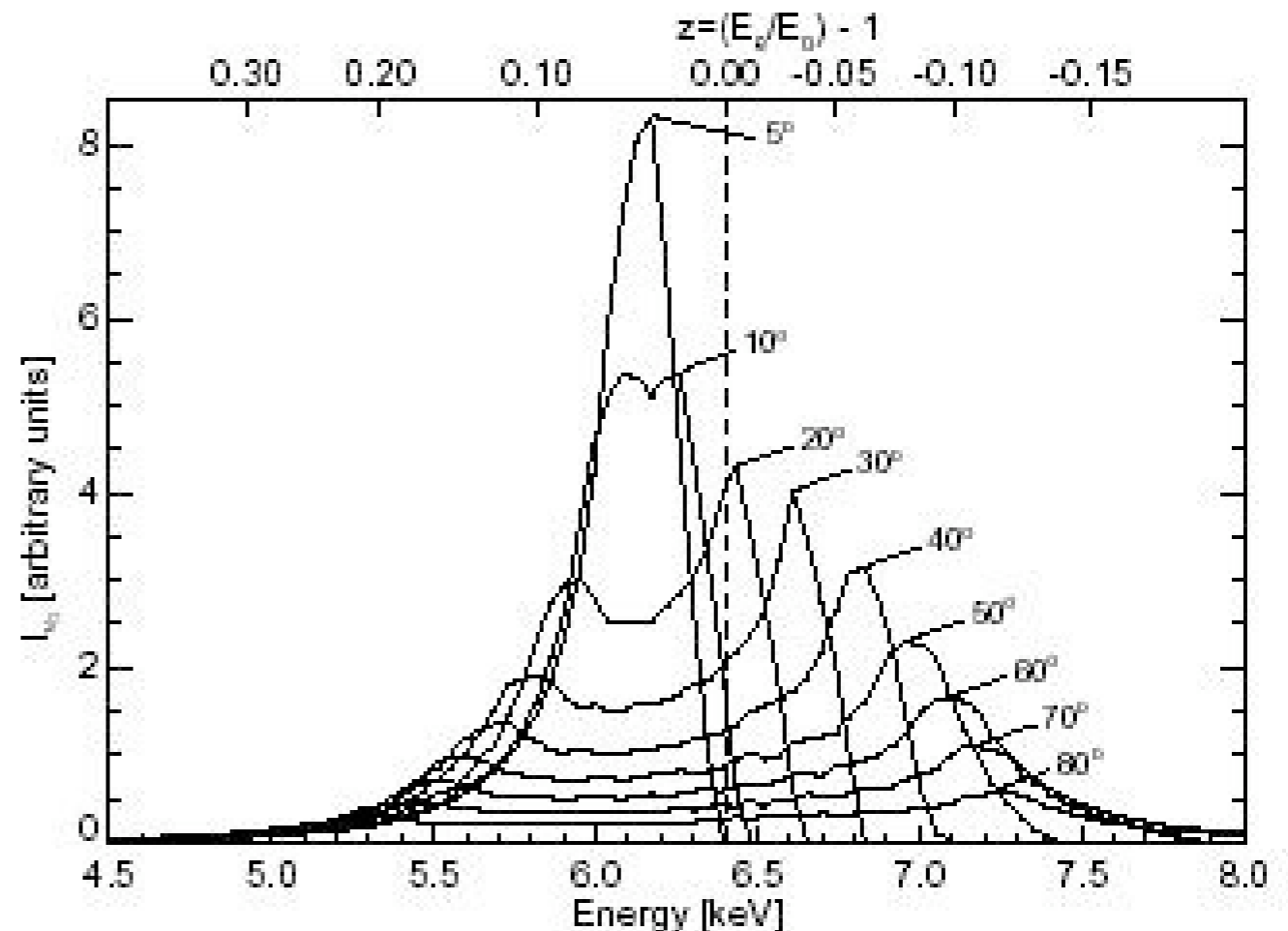
- ➔ Real disk atmospheres are much more complex. To determine their structure, we must model their radiative transfer, calculate thermal and ionization balance of each fluid element, and take into account MHD and effects from radiation pressure.
- ➔ Next step beyond fixed density is to assume hydrostatic equilibrium (where density, temperature, and pressure are constant).
- ➔ In the hydrostatic equilibrium case, thermal ionization instability arises. TII is the phenomenon that happens when pressure is specified and multiple thermal and ionization equilibria exist. Thus, very hot regions can coexist with cool regions while in pressure equilibrium.
- ➔ When modeling real reflection spectra, constant density models can be used with different inferred reflection fractions and ionization parameters.

# *Relativistic Effects*



# *Profile Dependence on Inclination*

- ➔ The influence of relativistic effects depends on the observer's inclination angle.
- ➔ For a disk seen face-on ( $i = 0^\circ$ ), gravitational/time-dilation redshifts dominate.
- ➔ At larger inclinations, line-of-sight Doppler effects dominate, and lines become broader.





## *Calculating Observed Line Flux*

- The specific flux  $F_{\nu_o}$  at frequency  $\nu_o$  as seen by an observer at infinity is the sum of the observed specific intensities  $I_{\nu_o}$  from all parts of the disk:

$$F_{\nu_o} = \int_{\Omega} I_{\nu_o} \cos \theta \, d\Omega \quad (1)$$

where  $\Omega$  is the solid angle subtended by the accretion disk, and  $\theta$  is the angle between the directions of the disk and the observed photon.

- Doppler boosting and gravitational redshift cause emitted and observed frequencies to differ by a factor  $g$ :

$$g = \frac{\nu_o}{\nu_e} = \frac{1}{1+z} \quad (2)$$

relating the observed frequency  $\nu_o$  and the emitted frequency  $\nu_e$  to redshift  $z$  of the photon.

# *Calculating Observed Line Flux*

→ Density of photons is constant along photon path and proportional to  $I(\nu) / \nu^3$ . Therefore, eq. (1) becomes:

$$F_{\nu_o} = \int_{\Omega} \frac{I_{\nu_o}}{\nu_o^3} \nu_o^3 d\Omega = \int_{\Omega} \frac{I_{\nu_e}}{\nu_e^3} \nu_o^3 d\Omega = \int_{\Omega} g^3 I_{\nu_e}(r_e, i_e) d\Omega \quad (3)$$

and computation of the spectrum depends on the value  $g \equiv \frac{\nu_o}{\nu_e}$

→ Calculation of observed flux can be done for weak-field & Schwarzschild metric or the strong-field Kerr metric.

→ Calculation can be done two ways:

- 1) Direct integration of the photon trajectory in each metric
- 2) Use the equation

$$F_{\nu_o} = \int T(r_e, i_e, g) I_{\nu_e}(r_e, i_e) dg r_e dr_e \quad (4)$$

and integrate over all values of  $g$  and the entire surface of the disk. The transfer-function  $T$  includes all relativistic effects.

## *Computing Line Profiles*

➔ To compute line profiles, we assume a geometrically thin, optically thick Keplerian accretion disk as the source of line radiation.

➔ Local emissivity of the line on the disk is parametrized as

$$I_{\nu e}(r_e, i_e) \propto f(i_e) r_e^{-\beta}$$

where  $f$  models different limb-darkening scenarios.

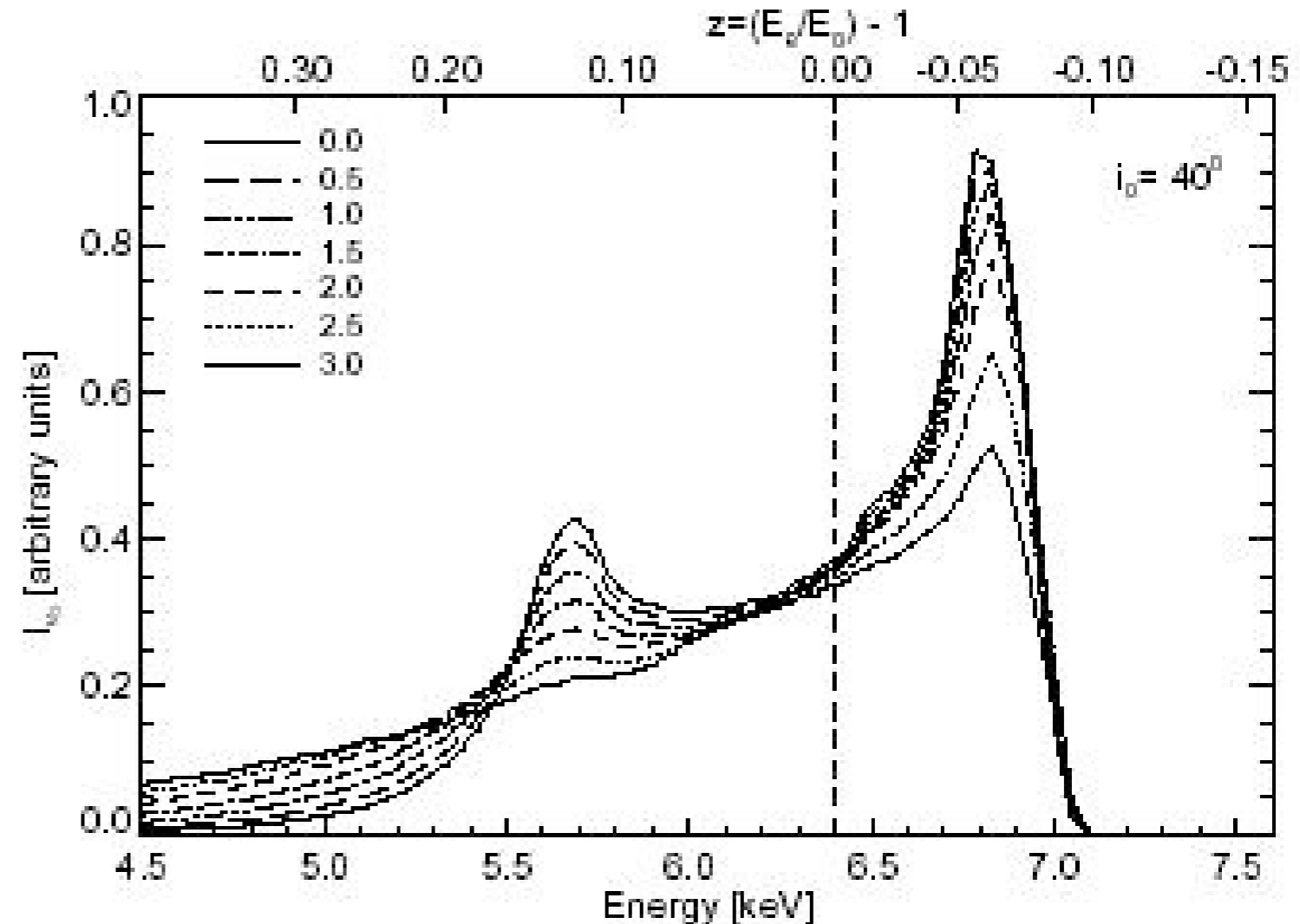
➔ Emitting part of the disk is assumed to go from the radius of marginal stability  $r_{\text{ms}}$  (radius of last stable orbit) to  $50 GM/c^2$

➔ For  $\beta > 2$ , outer limit doesn't matter since emission is dominated by inner regions of the disk.

➔ For  $\beta < 2$ , outer limit matters because emission originates from the outer region of the disk.

# *Profile Dependence on $\beta$*

- Line profiles change for different values of the emissivity coefficient  $\beta$ .
- For large  $\beta$ , most of the line emission takes place close to the last stable orbit.
- For small  $\beta$ , red wing of the profile gets weaker and practically undetectable.

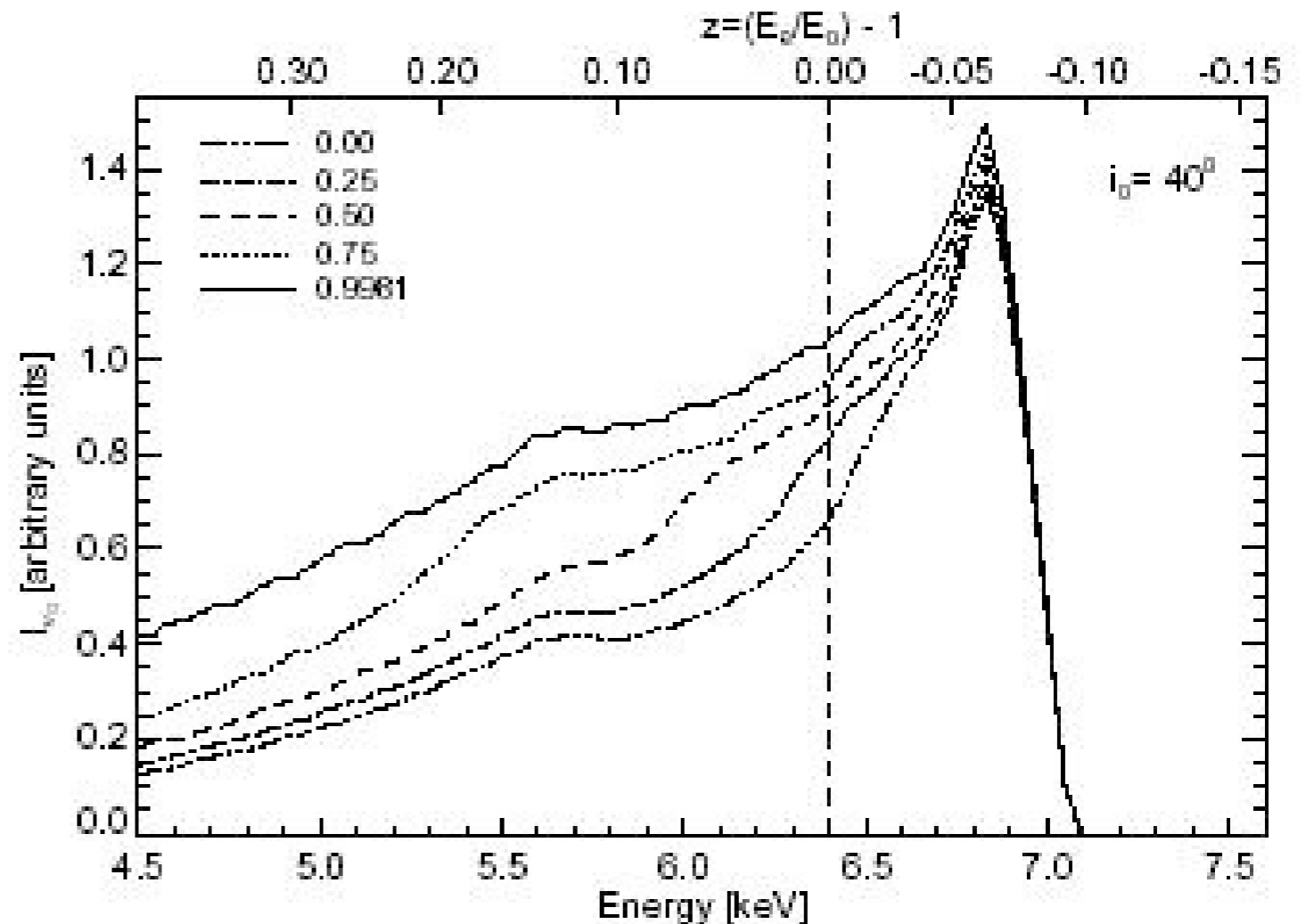




# *Profile Dependence on Spin*

→ Since we assume line emission extends to  $r_{\text{ms}}$ , and  $r_{\text{ms}}$  depends on black hole spin, the line profile also depends on spin.

→ Notice red-wing of the profile can extend to lower energies for rapidly-rotating black holes versus non-rotating black holes.



# *Iron Lines in AGN*

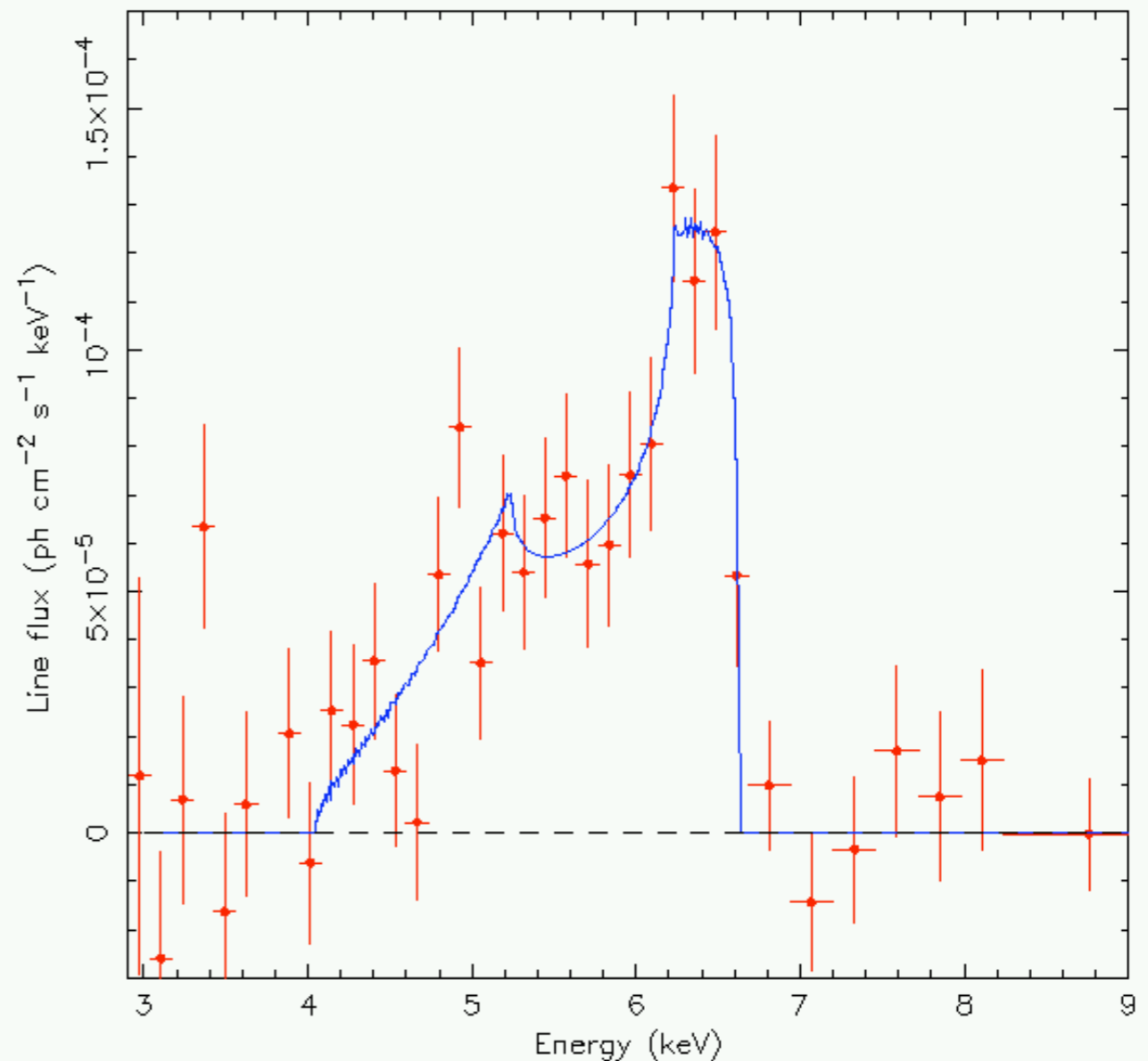
AGN give the cleanest observed relativistic iron lines for three reasons:

- 1) the primary X-ray continuum is often very featureless and easy to subtract to identify disk reflection signatures.
- 2) AGN accretion disks are not strongly ionized
- 3) GBHCs typically lie in the plane of the Galaxy, so they are usually much more heavily absorbed.



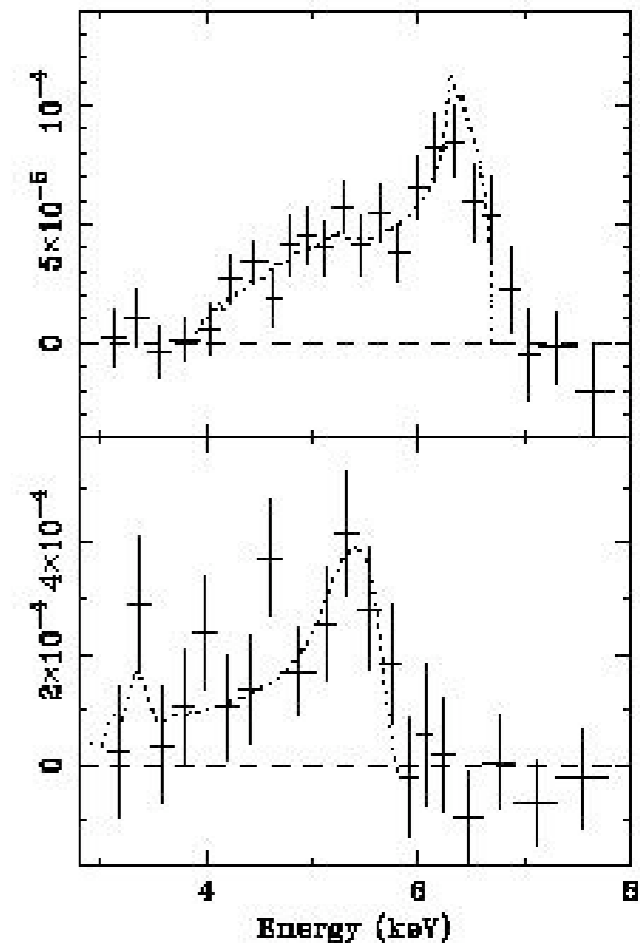
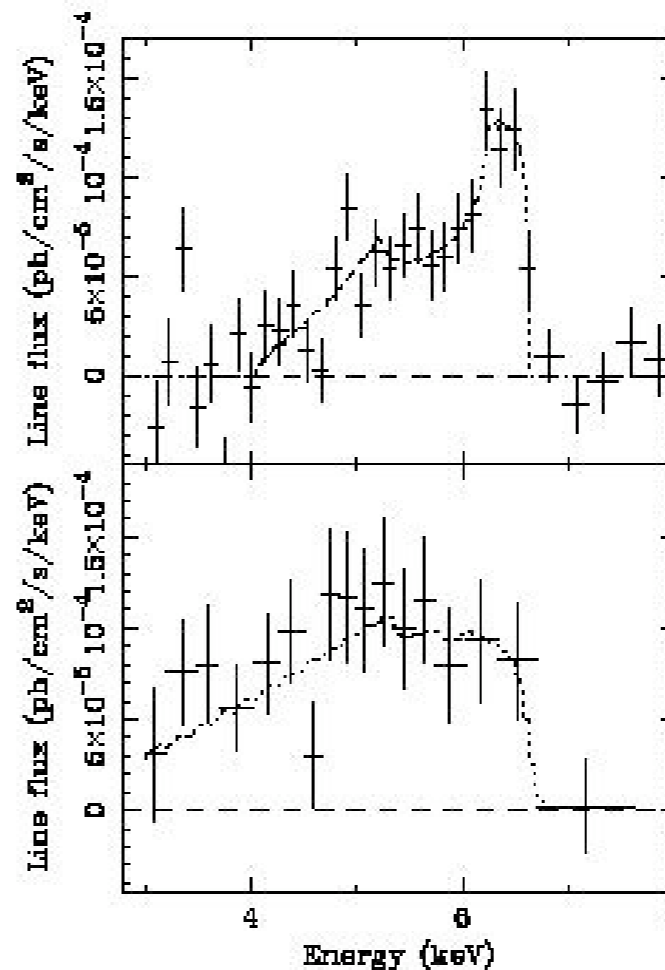
## *Iron Lines in AGN*

- ➔ MCG-6-30-15 was the first AGN where X-ray reflection from neutral material was clearly detected (using *EXOSAT* and *Ginga*)
- ➔ MCG-6-30-15 is a Seyfert I galaxy with a redshift  $z = 0.008$
- ➔ Mass of MCG-6-30-15 is poorly determined. Thus, astrophysical conclusions from study of line profiles are robust.
- ➔ *ASCA* observation confirmed the presence of a broadened iron line with  $E_0 = 6.2$  keV.
- ➔ Line profile best-fit with line emission from a Schwarzschild black hole with  $i = 27^\circ$ .



# *Iron Line Variability*

- ➔ Subsequent *ASCA* observations revealed iron line flux and profile dramatically changes with time.
- ➔ In a 1994 observation (left), a very broad profile was detected, with a pronounced red-wing.
- ➔ Dubbed a “deep minimum” state, the continuum flux fell below by average by a factor of 2-3, and the  $K\alpha$  line became much stronger and broader.
- ➔ In a 1997 observation (right), line emission was shifted to energies below 6 keV.
- ➔ Both can be explained via a large gravitational redshift in small radii on the accretion disk (line emission from within  $r = 6M$ ).



## *Radiation from Within $r_{ms}$ ?*

- ➔ If we assume no fluorescent emission line exists within  $r_{ms}$ , the DM spectrum requires a rapidly rotating black hole in order to have  $r_{ms}$  less than  $6M$ .
- ➔ In the case of MCG-6-30-15,  $a > 0.94$  if iron flux is distributed across the disk.
- ➔ However, if any region of the disk is allowed to produce observable line emission (including  $r < r_{ms}$ ) it is possible to produce arbitrarily large redshifts.
- ➔ So, the question arises: how much emission and reflection will occur from the plunging region of the disk?

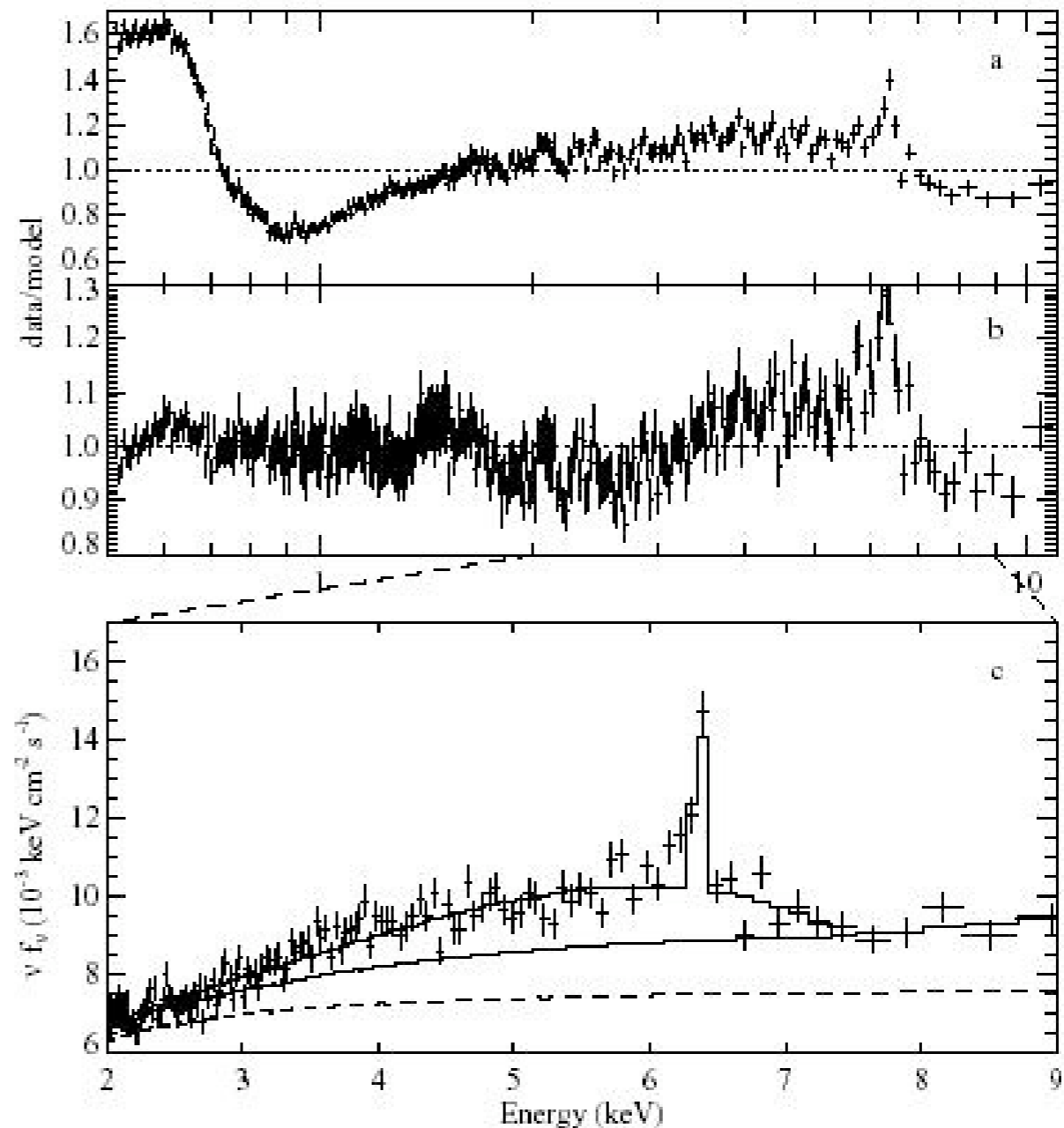
## *Radiation from Within $r_{ms}$ ?*

- ➔ The standard model for black hole accretion maintains the plunging region cannot support an X-ray active corona because there is no angular momentum transport and no dissipation of energy within the region.
  
- ➔ However, two cases exist which may allow appreciable X-ray reflection in the plunging region:
  - 1) The outer disk corona is geometrically thick, allowing it to irradiate the plunging region.
  - 2) The accretion flow at  $r < r_{ms}$  may dissipate a significant fraction of its binding energy, creating an inner corona responsible for X-ray reflection within the plunging region.



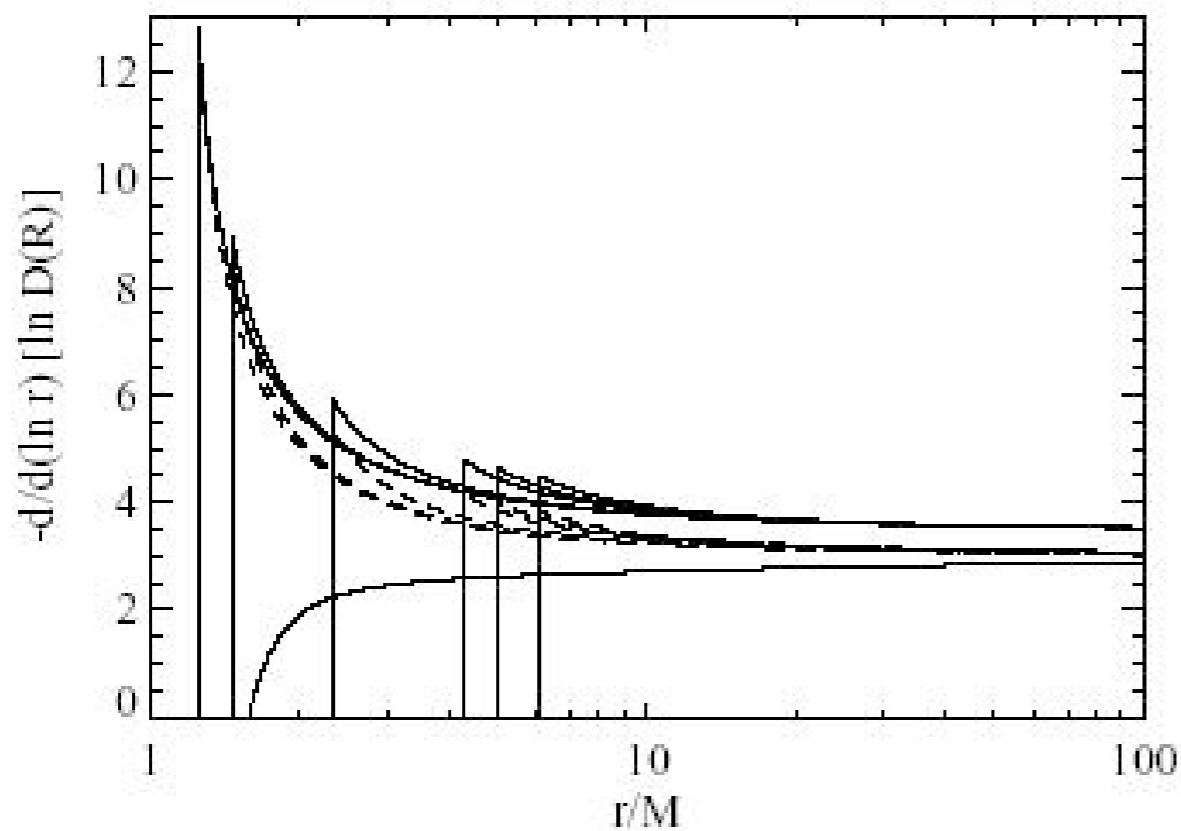
# *XMM-Newton Studies of MCG-6-15-30*

- ➔ Follow-up studies of MCG-6-15-30 with XMM-Newton confirmed the *ASCA* results and conclusions.
- ➔ X-ray reflection features were very broad and strong, requiring reflection within  $r = 6M$ .
- ➔ Assuming a near-extremal Kerr black hole ( $a^* = 0.998$  and  $r_{\text{ms}} = 1.23M$ ), the data constrain the inner edge of the reflecting region to  $r < 2M$  and a steep emissivity profile of  $4.5 < \beta < 6$
- ➔ If modeled as a Schwarzschild black hole, the inner edge of the reflecting region is constrained to  $r < 3M$  and a large emissivity index of  $\beta > 10$ .



# *Energy from Black Hole Spin*

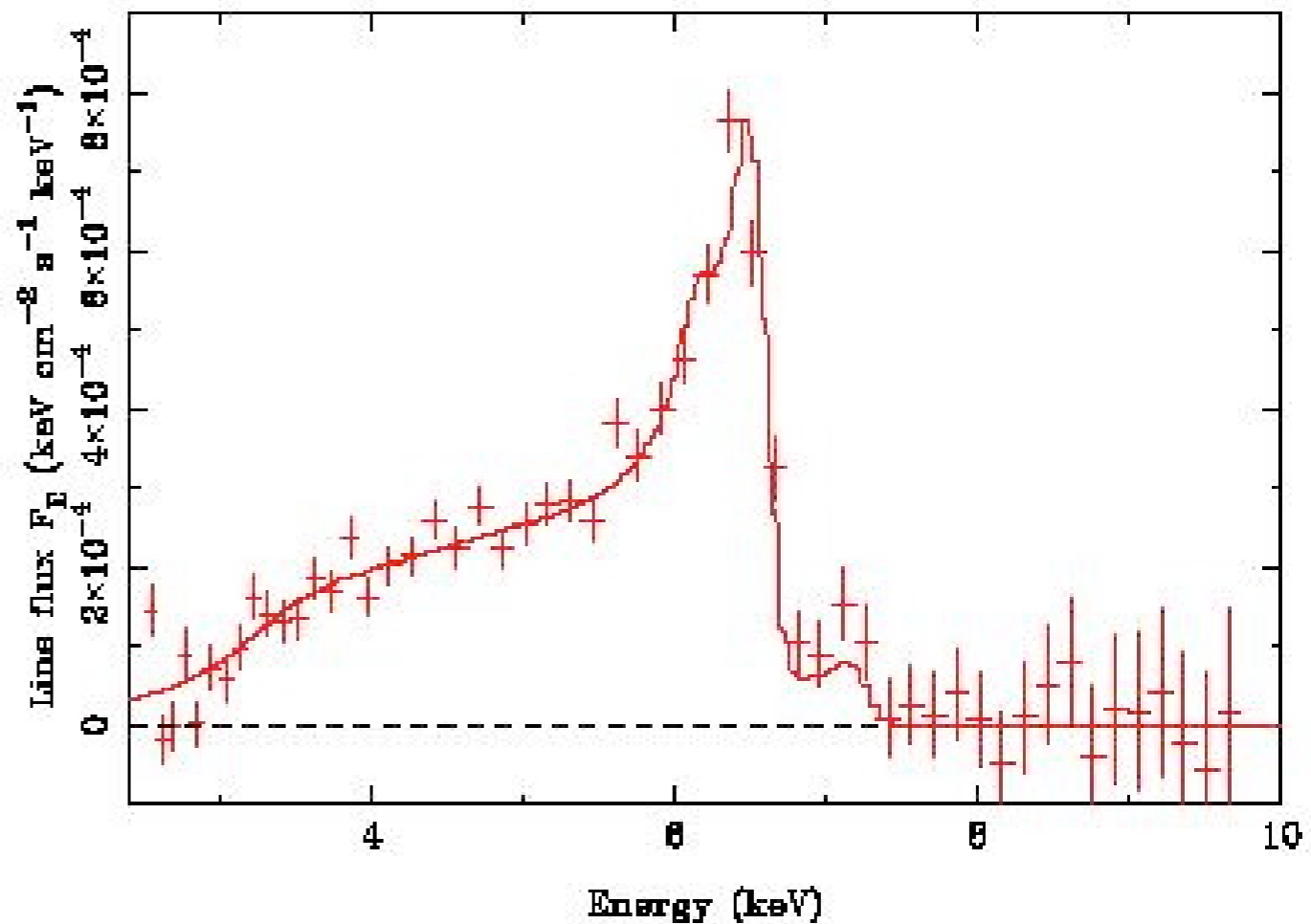
- ➔ Assume little to no X-ray reflection from within the plunging region.
- ➔ Assume local intensity of X-ray reflection from the disk surface is proportional to local dissipation in the underlying disk (true if ionization is uniform with radius).



- ➔ To account for increased flux in inner regions of the disk, significant enhancement of energy dissipation in these regions is necessary.
- ➔ Magnetically-induced torques at  $r_{ms}$  can enhance the amount of dissipation in these inner regions.
- ➔ Only rapidly-rotating black holes display the necessary dissipation profile, and extra energy must be directly derived from the BH spin.

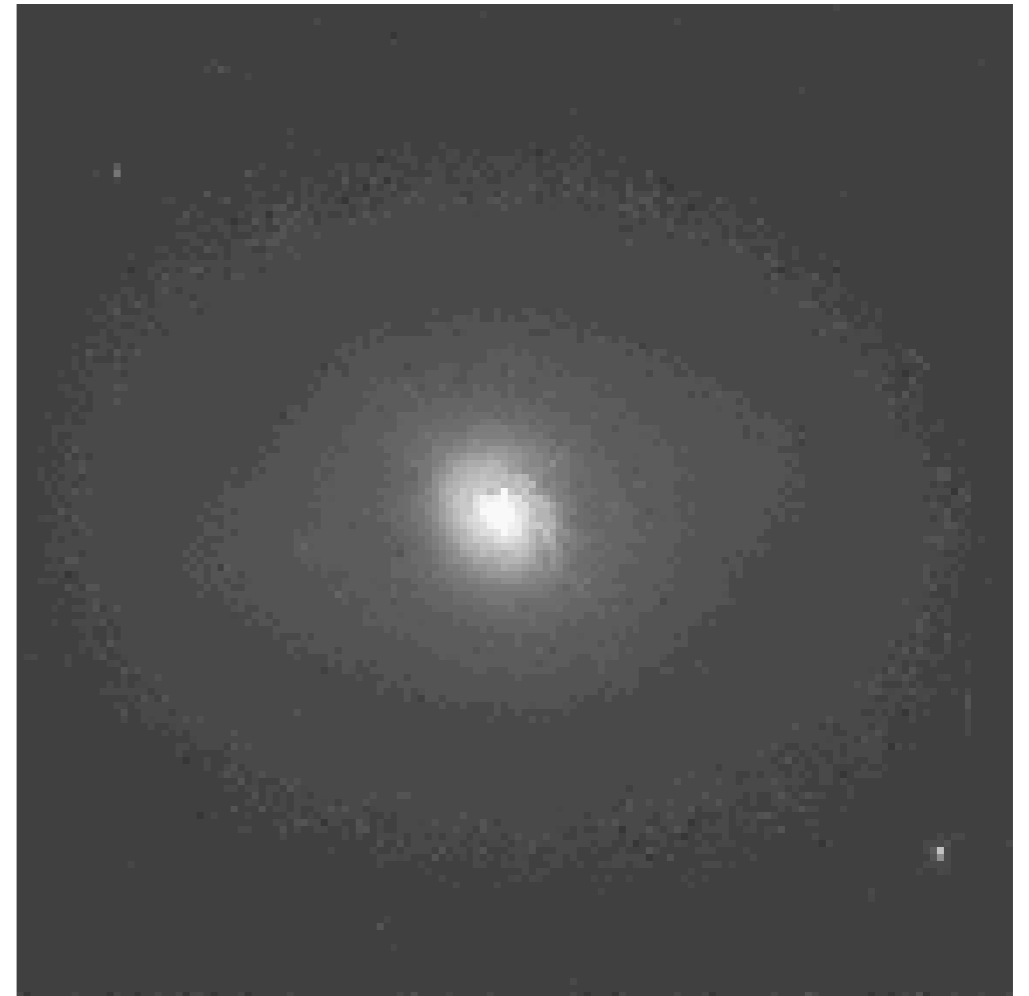
# *A New XMM-Newton Study*

- ➔ A recent 400 ks *XMM-Newton* observation of MCG-6-30-15 produced the best iron profile yet.
- ➔ A prominent blue horn indicates emission originates from larger radii within the disk than from the first observation.
- ➔ Extreme red-wing requires a steep emissivity profile.
- ➔ Still awaiting further analysis.



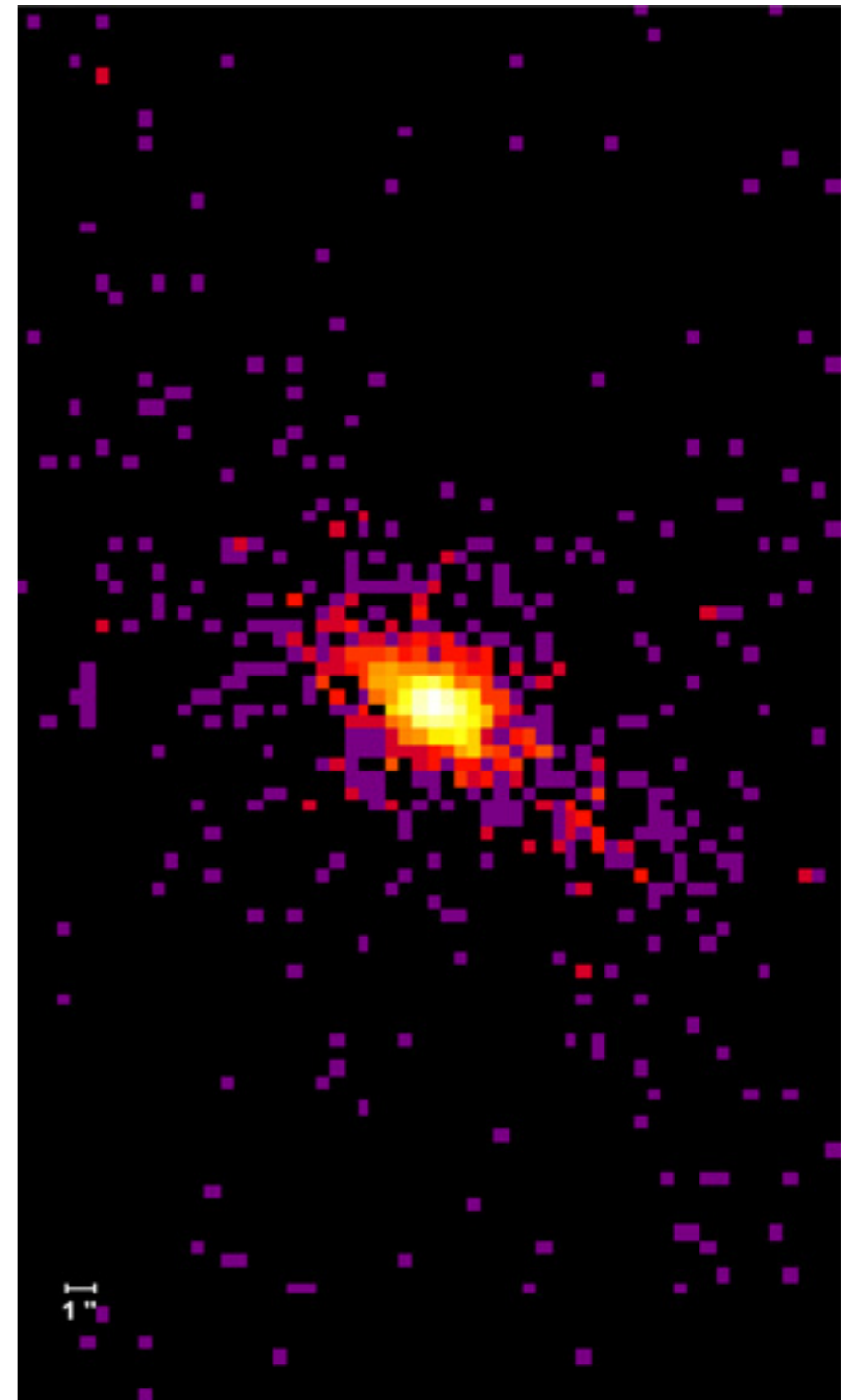
## *Other Seyfert Galaxies: NGC 3516*

- ➔ First observed with *ASCA*, NGC 3516 shows a red-wing of the iron line which tracks changes in the continuum flux.
- ➔ The blue-wing of the iron line displays variability uncorrelated with changes in the continuum flux, indicating complex patterns of fluorescence across the disk.
- ➔ *ASCA* data suggests the presence of an absorption line at 5.9 keV. This feature may be a sign of redshifted resonance absorption by ionized iron in plasma above the disk.



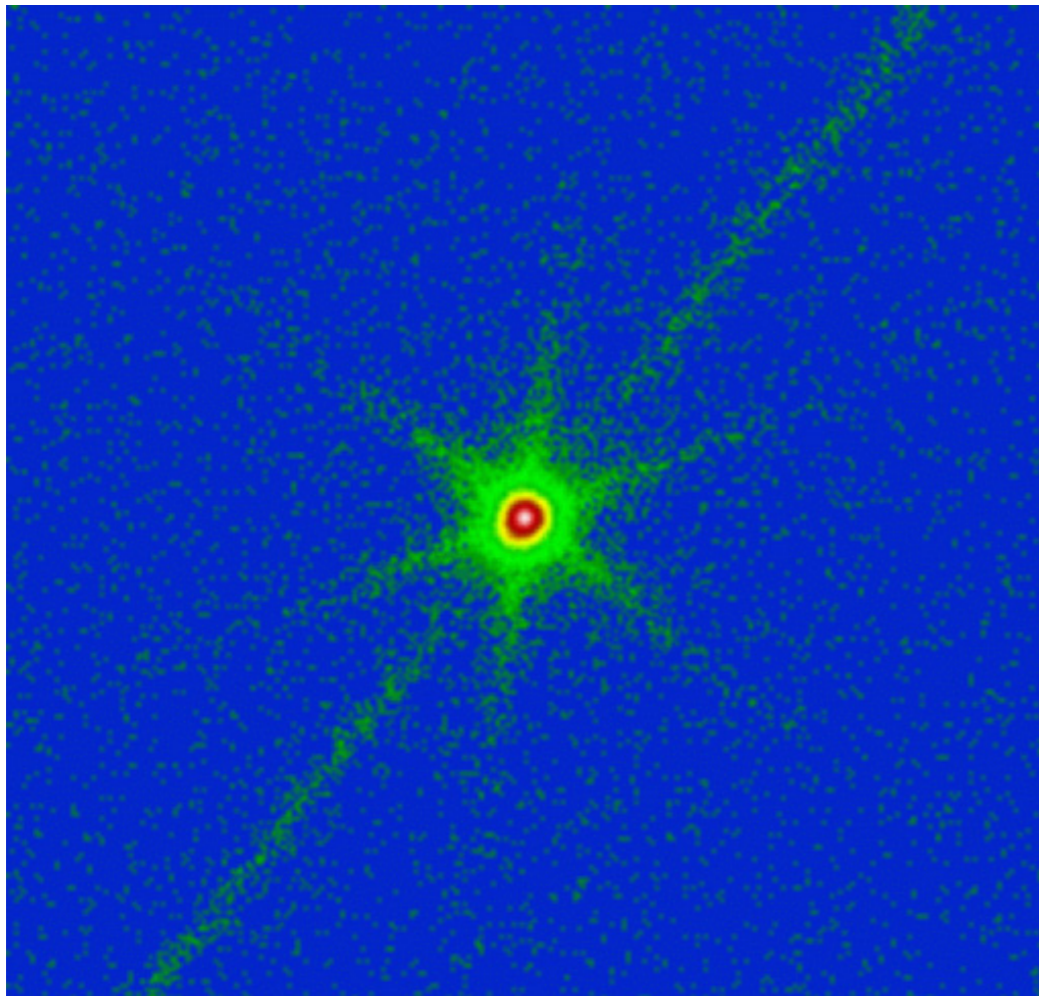
## *Other Seyfert Galaxies: NGC 4151*

- ➔ NGC 4151 also displays complex variability within the line profile.
- ➔ During a May 1995 *ASCA* observation, the iron line profile displayed red-wing variability with minor changes in the observed continuum.
- ➔ In a May 2000 observation, the continuum underwent significant variability and the iron line remaining relatively constant.
- ➔ These observations make it evident that the iron line in a given AGN can change its variability behavior.





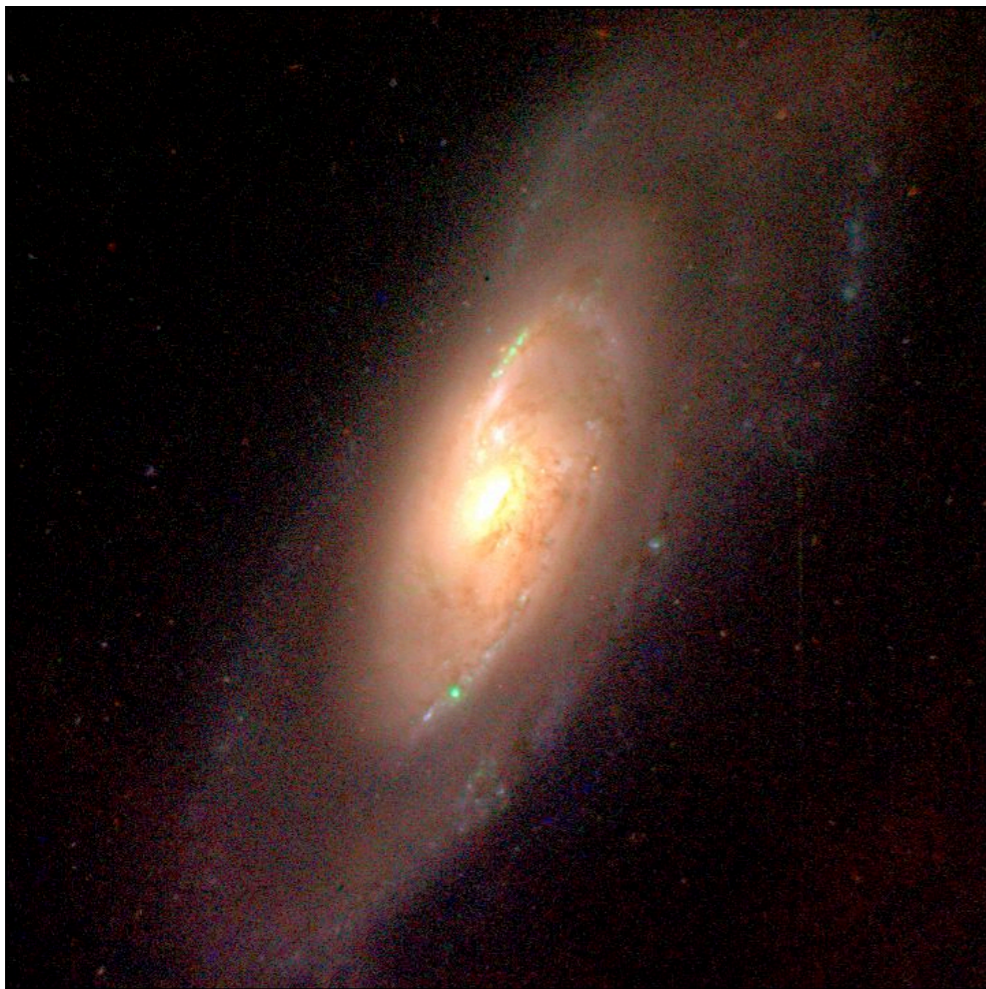
## *Other Seyfert Galaxies: NGC 5548*



- ➔ NGC 5548 displays a very narrow iron line: the line emitting region of the disk has an inner radius of  $r = 10M$ .
- ➔ However, the *Chandra* HETGS revealed a “narrow” core to the line originating through fluorescence of material far from the black hole.
- ➔ The large equivalent width of the narrow core indicates the material subtends a large part of the sky.
- ➔ Consequently, data are consistent with a relativistic accretion disk extending to the radius of marginal stability.

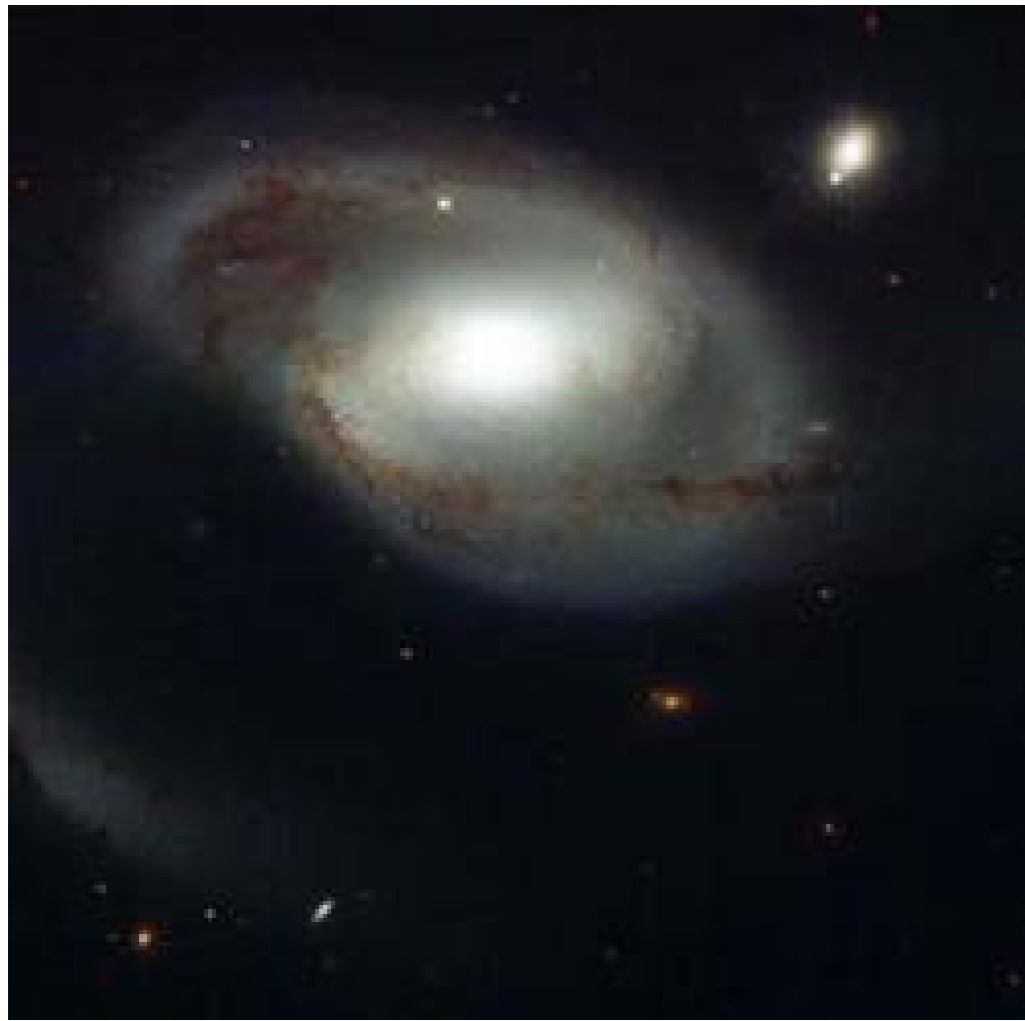


## *Low-Luminosity AGN*



- LLAGN are sources with a total radiative luminosity of  $L < 10^{42} \text{ erg s}^{-1}$ .
- Hard to observe since they are faint X-ray sources.
- NGC 4258, a well studied LLAGN, shows a narrow iron line, implying most of its fluorescent emission originated at  $r > 100M$ .
- With a large equivalent width, line likely originates from the disk itself, so the X-ray emitting corona must be extended.
- Studies of other LLAGN do not detect a broadened iron line, but they could be hiding in noise.

# *High-Luminosity AGN*

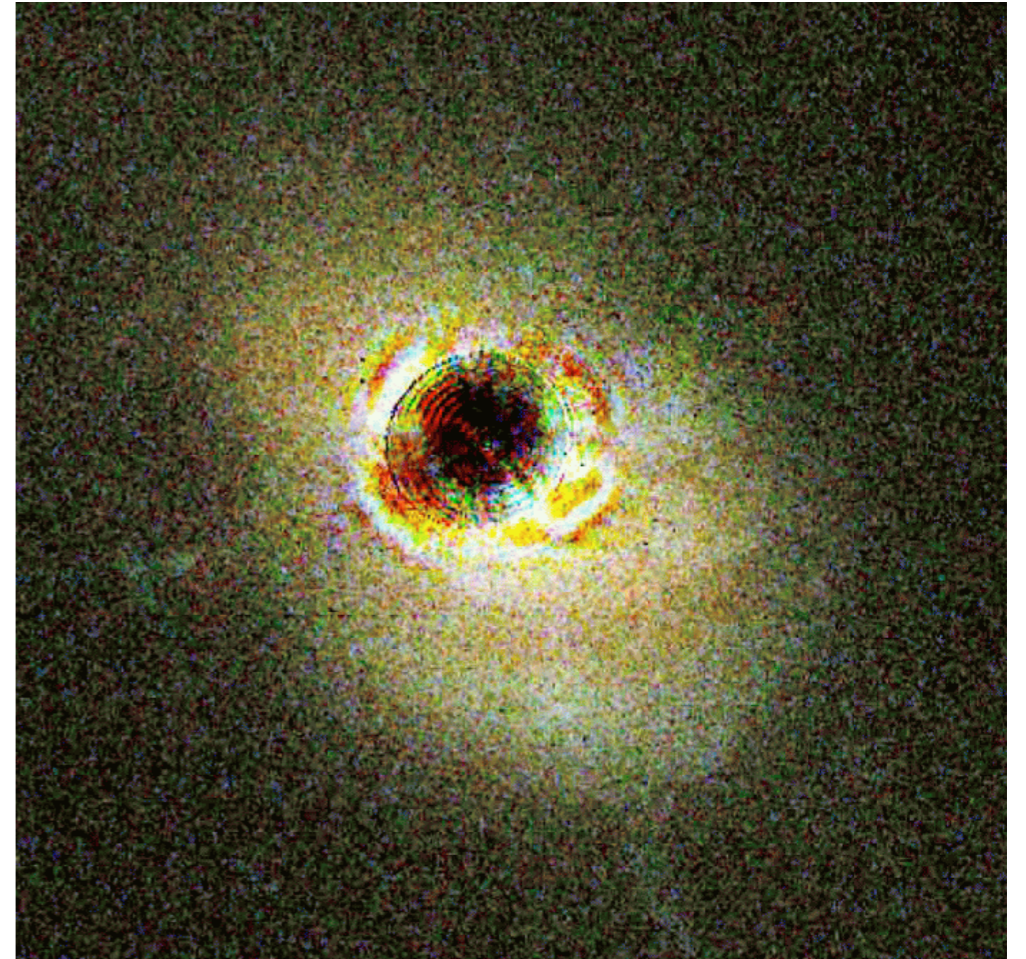


- ➔ Broad iron lines become appreciably weaker when X-ray luminosity reaches  $L_X \sim 10^{44} - 10^{45} \text{ erg s}^{-1}$ .
- ➔ Possible explanation: HLAGN possess more highly ionized accretion disks, an expected result if luminosity is determined by the Eddington fraction.
- ➔ Recent observations of Mrk 205 and Mrk 509 with *XMM-Newton* find broadened iron lines and energies corresponding to He-like and H-like iron.
- ➔ These observations likely are direct detections of ionized accretion disks.



## *Radio-Loud AGN*

- ➔ A big mystery in AGN research is the physics underlying radio-quiet versus radio-loud sources.
- ➔ Study of relativistic iron lines within these systems could allow comparison of the central structures and facilitate direct probing of the inner accretion disk.
- ➔ Observational constraints make studies of RL AGN difficult.
- ➔ Initial studies show broad iron lines and reflection continua are generally weak or absent in radio-loud sources
- ➔ Possible explanations: swamping of a spectrum by a beamed jet component, the inner disk might be very hot and have optically-thin radiatively-inefficient accretion flow, or it may be very highly ionized.

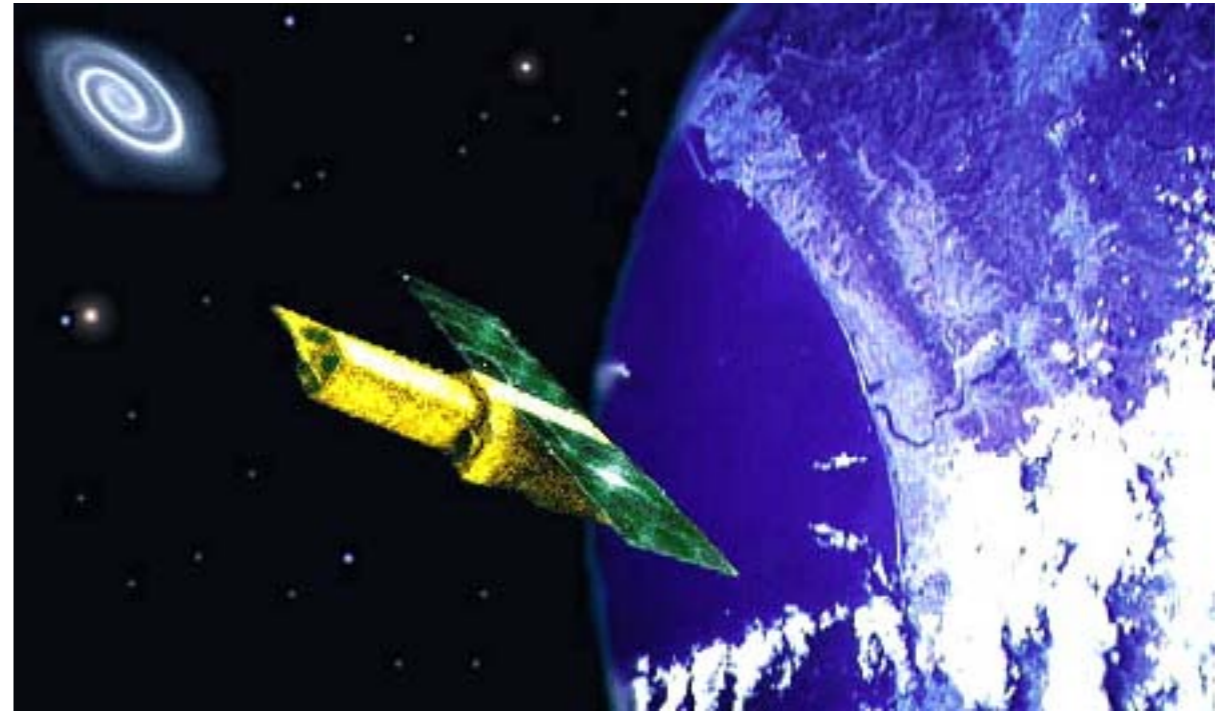


# *The Future of Iron Line Studies*

- ➔ With the continued operation of *XMM-Newton*, *RXTE*, and *Chandra*, data on X-ray reflection will gradually be collected for the different classes of black holes in the nearby universe.
- ➔ This data will allow the first observational investigations of black hole spin from GBHCs to AGN.
- ➔ Further investigation of variability in the iron line profiles will be studied on timescales down to  $\sim 10$  orbital periods.
- ➔ Future studies may also provide the first constraints on the environments of super-massive black holes at high redshift.

# *The Future of Iron Line Studies*

- ➔ After launch in 2005, *Astro-E2* will be able to study broad iron lines at high S/N in the iron line band.
- ➔ Additionally, *Astro-E2* will better constrain the shape of the reflection continuum.
- ➔ In the next decade or two, *Constellation-X* and *XEUS* observatories will have much larger collecting areas, drastically increasing imaging and spectral sensitivity.
- ➔ These missions will obtain good X-ray spectra from high-redshift AGN, data to study spectral variability on time scales around the order of the light-crossing time of the black hole, and information to investigate the temporal power-spectrum of the X-ray variability in great detail.





## *Conclusions*

- ➔ X-ray spectroscopy currently provides the best method to explore the astrophysical environment in the immediate vicinity of accreting black holes.
- ➔ Surface layers of black hole accretion disks are expected to produce X-ray reflection signatures as a result of external, hard X-ray illumination from the disk corona.
- ➔ The most prominent feature is a fluorescent  $K\alpha$  emission line which is dramatically broadened from rapid orbital motion and strong gravity effects.
- ➔ Study of Seyfert galaxies with *ASCA* and *XMM-Newton* reveals a cold accretion disk extending to the radius of marginal stability.
- ➔ Evidence suggests this method can probe spin of black holes.
- ➔ Future studies are necessary to test if iron lines are good indicators for black hole spin, and to probe the physical state of accretion flow in all black hole systems.